Capacitative Detection of Phase Separation in ^{3}He-^{4}He Mixtures near the Tricritical Point

Melora Larson, John Panek, Al Nash, and Norbert Mulders*

Jet Propulsion Laboratory, California Institute of Technology, Pasadena, CA 91109
**Department of Physics and Astronomy, University of Delaware, Newark, DE 19716*

We have used two different types of capacitative sensors for detecting the phase separation boundary in ^{3}He-^{4}He mixtures. We have used a parallel plate geometry to make bulk concentration measurements, and we have developed inter-digital capacitors (IDC's) to make local concentration measurements. The IDC's were developed as part of our on going effort to study the tricritical point in the absence of acceleration. The IDC's should be well suited for making measurements of the phase separation on the ^{3}He rich side of the phase diagram where the minority ^{4}He rich phase will grow out from the walls. The resolution and advantages of these two types of sensors are presented below along with preliminary ground based measurements of the phase separation boundary taken with the IDC's.

1. INTRODUCTION

Tricritical points are among the few physical systems for which Renormalization Group theory produces exact predictions. Therefore, the tricritical point in the ^{3}He-^{4}He phase diagram offers many unique opportunities to test the understanding of critical phenomena.[1,2] In particular, all of the phase boundaries should appear linear in the temperature concentration plane approaching the tricritical point, with extremely weak logarithmic corrections. To fully test these predictions, the inhomogeneities introduced in the presence of gravity by the diverging concentration susceptibility must be removed by performing the experiment in a micro-gravity environment.[3]

Before an experiment to study the tricritical point can be fruitfully performed in the micro-gravity environment of an orbiting platform (like the

International Space Station), one must understand how the phase separation process will occur in the absence of the stabilizing influence of gravity. On the ^{4}He-rich side of the phase diagram, where the ^{3}He molar concentration, X, is less than the tricritical concentration, X_{tcp}=0.675,[1] the minority phase will grow out of the ^{3}He enriched liquid-vapor interface at the bubble.[8] If the cell is appropriately designed to have a vapor bubble outside the measurement volume, there will be a range in temperature over which the sample cell contains only the ^{4}He-rich component of the phase separated mixture. In contrast, on the ^{3}He-rich side of the phase diagram ($X > X_{tcp}$) phase separation will start with the formation of a macroscopically thick ^{4}He-rich surface layer,[4] filling the sample cell with layers of both phases. This understanding of the phase separation process implies that while a global concentration sensor would be appropriate for observing phase separation on the ^{4}He rich side, a sensor sensitive to the concentration near the cell walls would be more appropriate to use on the ^{3}He rich side.

We are developing capacitors as concentration sensors since the mixture's dielectric coefficient, ϵ, depends on the concentration. The close relationship between the concentration and the dielectric constant makes it possible to detect phase separation as a sharp kink in the dielectric constant. When the sample is cooled down, on phase separation the mixture is constrained to follow the phase separation curve instead of continuing along a path of constant concentration. We use parallel plate capacitors to measure the global concentration in our sample cell and inter-digital capacitors (IDC's) to sense the surface layer concentration. The remainder of this paper focuses on the IDC's we have developed, giving their specifications along with a comparison to our measurements using parallel plate capacitors. We also present the data from our preliminary ground based phase separation studies using IDC's .

2. INTER-DIGITAL CAPACITORS

The IDC's we have developed consist of an array of equally spaced interpenetrating electrode fingers (see Figure 1). The spacing between the fingers equals the width of the individual fingers. The capacitors were produced using standard lithography techniques to pattern a 300nm thick gold layer evaporated on top of a chrome coated single crystal quartz substrate. IDC's of two different configurations were manufactured: 80 fingers 50μm wide with an 8mm overlap and 76 fingers 20μm wide with a 3mm overlap. A total of four sensors were deposited on the substrate, three 20μm capacitors, arranged in an equilateral triangle around one 50μm sensor (see Figure 1).

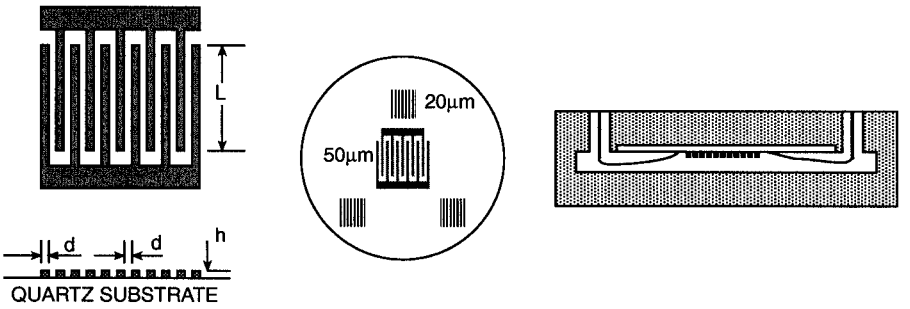

Fig. 1. Schematic representation of our IDC and sample cell. The IDC has a finger width, d, equal to the finger spacing. For our sensors, h=0.3μm, (d=50μm, L=8mm) and (d=20μm, L=3mm). There are a total of 4 sensors, one 50μm, and three 20μm sensors per substrate. Note that the IDC's are mounted on the top surface of the pancake volume in the copper cell.

The capacitance of an IDC can be analyzed by defining a unit cell consisting of a pair of electrode fingers. Then the total capacitance is just the sum of the capacitance, C_{uc}, of all the parallel unit cells created by the N fingers: $C = L(N-1)C_{uc}$. The capacitance of each unit cell can be further decomposed into three parallel capacitors: C_{F-Q} (capacitance of the fingers in the lower half plane containing the quartz substrate), C_{F-He} (capacitance of the fingers in the upper half plane), and C_{gap-He} (capacitance of the gap region between the fingers). The capacitance of the fingers has been calculated using conformal mapping[6] to be given by:

$$C_{F-Q}+C_{F-He} = \epsilon_0 \frac{\epsilon_Q + \epsilon_{He}}{2} \frac{K[(1-(d/2d)^2)^{1/2}]}{K[d/2d]} = 0.6396\epsilon_0(\epsilon_Q+\epsilon_{He}) \quad (1)$$

where $K[x]$ is the complete elliptic integral of the first kind. The capacitance in the gap volume between the fingers can be treated as a plate capacitor:

$$C_{gap-He} = \epsilon_0 \epsilon_{He} \frac{h}{d}. \quad (2)$$

In contrast to the parallel plate geometry, the capacitance of the IDC is strongly influenced by the substrate the capacitor is deposited on as can be seen from equation 1. Because the dielectric coefficient of the quartz is significantly larger than that of the helium (about 3.4 versus 1.05), the contribution from C_{F-Q} is the largest component of the total capacitance. Also, the dielectric coefficient of quartz is temperature dependent. Therefore, the empty cell capacitance must be measured as a function of temperature to extract the dielectric coefficient of the helium from the filled cell data.

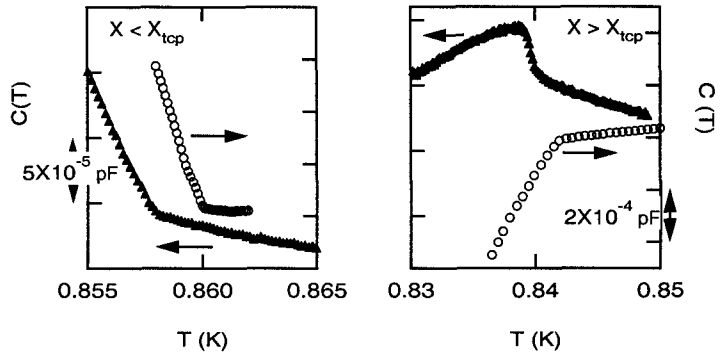

Fig. 2. Comparison of IDC (solid triangles, left scale) and parallel plate (open circles, right scale) data for phase separation on the helium-4 rich side of the coexistence curve ($X = 0.64$ (IDC) and 0.65 (plate)), and on the helium-3 rich side ($X \approx 0.69$, $X_{IDC} > X_{plate}$).

The sensitivity of the IDC to changes in the helium dielectric can be calculated from equations 1 and 2. Neglecting small corrections, the sensitivity can be written as:

$$\frac{\partial C}{\partial \epsilon} = (0.32)\epsilon_0 \frac{A}{d} \tag{3}$$

where $A = d * L * (2N - 1)$, is the active area of the IDC. Equation 3 shows that the sensitivity of the IDC is about one third the sensitivity of a parallel plate capacitor with the same overall area and a plate spacing equal to the IDC finger spacing.

One of the desirable features of an IDC is its sensitivity to only a small volume near the capacitor. Numerical modeling of a capacitor similar to the ones used here showed that the capacitors are sensitive only to a region within 1/3 to 1/2 the finger width, d.[7] So, for an appropriate choice of d, the dielectric coefficient of a few μm thick surface layer can be measured. This is in contrast to a parallel plate capacitor where a thin surface layer would be averaged out unless the cell was of a size comparable to the surface layer.

3. EXPERIMENTAL RESULTS

The experimental cell used was a copper cell consisting of a lower pancake shaped volume, 127μm tall, and a larger upper volume containing the wire feed throughs and vapor bubble. The substrate containing the IDC's was epoxied flush into the top of the pancake region of the cell (see figure

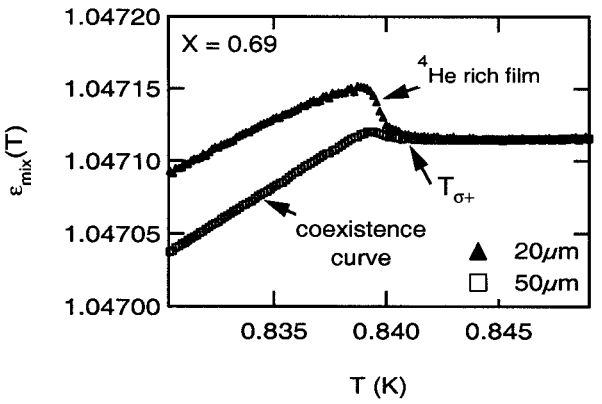

Fig. 3. Dielectric coefficient at phase separation for a representative 20μm and the 50μm IDC sensors. Notice that the 50μm sensor is less affected by the growth of the helium-4 rich film.

1). The IDC's were placed away from the bottom of the cell so that the formation and growth of the helium-4 rich film on the helium-3 rich side of the phase diagram could be observed separated from the bulk phase separation.

Raw capacitance data at phase separation for one of the 20μm IDCs is shown in figure 2. Also shown in figure 2 is data taken using a parallel plate capacitor with a spacing of 160μm and an area of 1.8cm^2. As can be seen from the scales for the two traces and the initial slopes after phase separation, the observed sensitivity of the IDC is almost 8 times less than that of the parallel plate capacitor. This lower sensitivity for the IDC is consistent with equation 3 and the geometry of the capacitors.

More interesting than the sensitivity of the two capacitors is the qualitative behavior at phase separation. For concentrations with concentration $X < X_{tcp}$, both capacitors show a sharp kink upward in their capacitance on cooling through phase separation as the capacitors measure the dielectric coefficient of the majority ^{4}He phase along the coexistence curve. For $X > X_{tcp}$ the parallel plate capacitor still shows a sharp kink as the mixture is cooled through phase separation (downwards this time since the ^{3}He rich phase is the majority phase). In contrast, at phase separation, the capacitance of the IDC initially increases as the ^{4}He surface layer grows. Once this surface layer has stabilized, the IDC capacitance starts to decrease and follow the dielectric coefficient of the majority, ^{3}He rich phase, along the coexistence curve.

The capacitance measurements of the IDC were converted into the di-

electric coefficient of the helium by correcting for the quartz background (measured with the cell empty) and verifying the coefficients of equations 1 and 2 at a temperature well above the coexistence curve where the mixture's dielectric coefficient is known.[5] Figure 3 shows the measured dielectric coefficient for a representative 20μm IDC's and the 50μm IDC. As can be seen from the figure, the effect of the ^{4}He film is much smaller for the 50μm than the 20μm. This difference is expected since the surface film's saturated thickness should be only a few μm's, which is a much smaller fraction of the active region of the 50μm IDC than the 20μm.

ACKNOWLEDGMENTS

This work was performed at the Jet Propulsion Laboratory under a contract with NASA.

REFERENCES

1. For an exhaustive review of static and transport properties of pure ^{4}He as well as isotopic mixture see: G. Ahlers, in *The Physics of Liquid and Solid Helium, Part 1*, K.H. Benneman and J.B. Ketterson eds, (Wiley, New York, 1976).
2. A more recent review of the transport properties is presented in: H. Meyer, *J. Low Temp. Phys.* **70**, 219, (1988).
3. M. Mohazzab, *et al.*, *J. Low Temp. Phys.* **113**, 1031 (1998).
4. J. -P. Romagnan, *et al.*, *J. Low Temp. Phys.* **30**, 425 (1978).
5. H. A. Kierstead, *J. Low Temp. Phys.* **24**, 497 (1976).
6. H. E. Endres and S. Drost, *Sensors and Actuators* **B 4**, 95 (1991).
7. J. S. Kim and D. G. Lee, *Sensors and Actuators* **B 30**, 159 (1996).
8. N. R. Brubaker and M. R. Moldover, *Low Temperature Physics-LT13* **1**, 612 (Plenum Press, 1974).